ASTRONOMY & ASTROPHYSICS
SUPPLEMENT SERIES

Astron. Astrophys. Suppl. Ser. **126,** 247-250 (1997)

Penetrating the "zone of avoidance"⋆

IV. An optical survey for hidden galaxies in the region $130^\circ \leq \ell \leq 180^\circ$, $-5^\circ \leq b \leq +5^\circ$

W. Saurer, R. Seeberger, and R. Weinberger

Institut für Astronomie der Leopold-Franzens-Universität Innsbruck, Technikerstraße 25, A–6020 Innsbruck, Austria

Received January 2; accepted January 23, 1997

Abstract. As the fourth part in a series of papers on galaxies in the "zone of avoidance" (ZOA) of the Milky Way we present a compilation of 1067 galaxies discovered during a systematic search on Palomar Observatory Sky Survey I (POSS I) red-sensitive prints. The region searched comprises 500 square degrees, at $130^\circ \leq \ell \leq 180^\circ$, $-5^\circ \leq b \leq +5^\circ$. In addition to galactic and equatorial coordinates, we list maximum and minimum optical diameters derived from both the red- and blue-sensitive prints and made cross checks with the IRAS PSC catalogue. An asymmetric distribution of the galaxies with respect to the galactic equator is found and is compared to the locations of optically visible dust clouds and/or the distribution of IR-emitting dust material. There is a pronounced bridge of galaxies across the galactic plane at $\ell \approx 160^\circ$ which will be discussed according to recent results on the extension of the Pisces-Perseus supercluster.

Key words: catalogs — (ISM): dust, extinction — Galaxy: structure — galaxies: clusters: Psc-Per supercluster — galaxies: general

1. Introduction

In the previous parts of our series (Weinberger et al. 1995: Paper I (literature search for all optical galaxies within $|b| \leq 5^\circ$); Seeberger et al. 1996: Paper II ($180^\circ \leq \ell \leq 240^\circ$, $-5^\circ \leq b \leq +5^\circ$); and Lercher et al. 1996: Paper III ($120^\circ \leq \ell \leq 130^\circ$, $-10^\circ \leq b \leq +10^\circ$)) we explained the considerable significance of studies of the extragalactic sky in the "zone of avoidance" (ZOA) of the Galaxy. Furthermore, we described our search methods, the material where our surveys for optically visible galaxies have been carried out, and presented extensive compilations including dicussions of our findings in selected regions. In other papers, we also demonstrated the usefulness of our data for investigations at 21 cm that led, e.g., to better insights in the radial velocity distribution of galaxies in the area $90^\circ \leq \ell \leq 110^\circ$, $-10^\circ \leq b \leq +10^\circ$ (Seeberger et al. 1994) or to the discovery of two close (≈3 Mpc) galaxies in the ZOA (Huchtmeier et al. 1995), the more massive of which was also discovered by Kraan-Korteweg et al. 1994).

In this installment we present 1067 galaxy candidates discovered during our search of 500 square degrees in the region $130^\circ \leq \ell \leq 180^\circ$, $-5^\circ \leq b \leq +5^\circ$ on POSS I E (red-sensitive) prints. This material, although slightly inferior compared to the new POSS II as to limiting magnitude, but distinctly inferior as to resolution (fine-grain emulsion of the latter) has still to be used for search purposes, since the POSS II is not fully available yet.

Our future installments will comprise the results of our optical searches of i) the areas $33^\circ \leq \ell \leq 80^\circ$, $-5^\circ \leq b \leq +5^\circ$ and will also include $110^\circ \leq \ell \leq 120^\circ$, $-10^\circ \leq b \leq +10^\circ$, ii) the area around the Circinus Galaxy $306^\circ \leq \ell \leq 316^\circ$, $-5^\circ \leq b \leq +5^\circ$, iii) the areas $20^\circ \leq \ell \leq 80^\circ$, $-10^\circ \leq b \leq -5^\circ$ and iv) $20^\circ \leq \ell \leq 80^\circ, +5^\circ \leq b \leq +10^\circ$.

2. Results and discussion

In Fig. 1, the distribution of our galaxy candidates is shown. Even at first glance, there are two obvious characteristics. First, one notices a pronounced preponderance in numbers of galaxies at negative galactic latitudes, from $130^\circ \leq \ell \leq 160^\circ$. Second, there appears to be a marked connection across the galactic plane, at $160^\circ \leq \ell \leq 165^\circ$ and an extended clump of galaxies at $165^\circ \leq \ell \leq 170^\circ, +2^\circ \leq b \leq +5^\circ$.

A cross-check with the distribution of dark nebulae of Lynds (1968) shows that the "holes" in the

Send offprint requests to: Walter.Saurer@uibk.ac.at

⋆ Table 1 is only available in electronic form at the CDS via anonymous ftp to cdsarc.u-strasbg.fr (130.79.128.5) or via http://cdsweb.u-strasbg.fr/Abstract.html

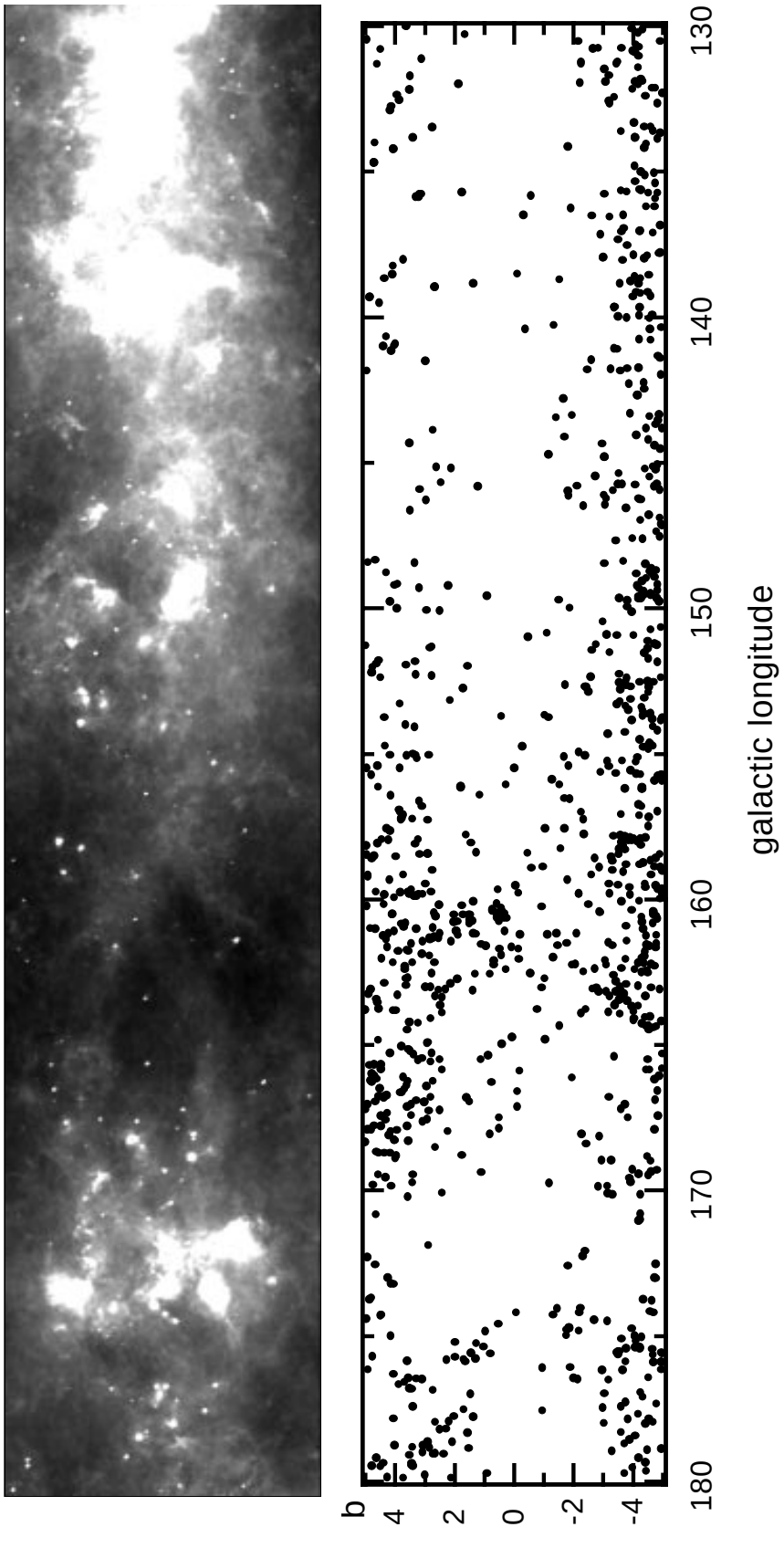

Fig. 1. Right: distribution of the new galaxies in galactic coordinates. Left: the 60 μ flux density taken from the IRAS Sky Survey Atlas; black (white) areas correspond to low (high) flux densities. Both parts of the figure represent the same region. (**To be seen in landscape**)

distribution (e.g. at $\ell \approx 133°$ and $\ell \approx 172°$) for the former location partly does, but for the latter one does not coincide with dust clouds. The above-mentioned preponderance might be related to the location of these (mostly nearby) obscuring clouds preferentially above the plane there. Anyway, the asymmetrical distribution in the region $130° - 160°$ is probably due to the existence of the galactic warp, evident as the bending of the dust layer (see also Freudenreich et al. 1994). In this context we found that the $60\,\mu$ (Fig. 1) or $100\,\mu$ IRAS sky flux densities that are an approximate measure of the total extinction in front of the galaxies (see Paper II), accord roughly with their distribution. In other words, the distribution appears to reflect the distribution of the galactic dust, and galaxy concentrations are rather holes or transparent locations in the dust layer than real clusters of galaxies. In the region $160° - 180°$ the distribution of the galaxies as well as the $60\,\mu$ IRAS flux densities appear to be symmetrical with respect to the galactic equator. The reason for this can be attributed to the crossing of the dustlayer with the galactic equator.

The excess of galaxies at about $\ell \approx 160°$ was first noted by Weinberger (1980) who called it a "striking conglomerate of galaxies". The bridge-like appearance in Fig. 1, across the galactic plane, however brings to mind the frequently raised question whether or not the main ridge of the Perseus-Pisces supercluster crosses the ZOA and connects to structures in the norther galactic hemisphere including the 3C 129 cluster at $\ell \approx 160°$ and $b \approx 0°$ (Hauschildt 1987) and cluster Abell 569 at $\ell \approx 170°$ and $b \approx +20°$ (Focardi et al. 1984; Chamaraux et al. 1990). According to new and extensive 21 cm measurements this problem appears to be settled: Lu & Freudling (1995) report that it is still possible that 3C 129 is connected to the main ridge of the PP supercluster, but a connection to Abell 569 can probably be ruled out. For the bridge in Fig. 1 this result consequently is not entirely conclusive: again it calls for further measurements, since Lu & Freudlings's conclusion obviously does not exclude at least a partial crossing, up to $b \approx 2 - 5°$.

In Table 1 our list of 1067 optical galaxy candidates is presented. The whole compilation is available from the SIMBAD database. The columns have the same meaning as in Paper III. Note that in this table the letters E and O correspond to the POSS I-E (red-sensitive) and POSS I-O (blue-sensitive) prints, respectively. Maximum and minimum diameters were determined and are presented in arcmin. In addition, mean average bulge (b) diameters are given. All diameters listed have an accuracy (of measurement) of ± 0.05 mm, but are presented in hundredths of arcmin to avoid biases that would occur in the course of rounding. A colon means that a galactic nature of the object cannot be excluded. An asterisk was used when more than one optical galaxy fell within the boundaries of one IRAS point source error ellipse.

In our previous papers we found that only a few percent of the optical galaxies turned out to have counterparts in the IRAS Point Source Catalogue. This holds true also for the galaxy sample presented in this paper. Since the IRAS two-colour distribution shows the same pattern as already shown and dicussed e.g. in Paper II, we will not repeat it here. The same applies for the presentation of the size distribution function that indicates a complete size limited sample down to a certain diameter limit (0.4 arcmin, see Fig. 6 in Paper II).

Acknowledgements. We would like to thank W. Jais for his help in the data acquisition. This work was supported by the "Fonds zur Förderung der wissenschaftlichen Forschung", project no. P 8325-PHY and by the "Jubiläumsfonds der Österreichischen Nationalbank", project No. 4713 (computer facilities).

References

Chamaraux P., Cayatte V., Balkowski C., Fontanelli P., 1990, A&A 229, 340
Focardi P., Marano B., Vettolani G., 1984, A&A 136, 178
Freudenreich H.T., Berriman G.B., Dwek E., et al., 1994, ApJ 429, L69
Hauschildt M., 1987, A&A 184, 43
Huchtmeier W.K., Lercher G., Seeberger R, Saurer W., Weinberger R., 1995, A&A 293, L33
Kraan-Korteweg R.C., Loan A.J., Burton W.B., et al., 1994, Nat 372, 77
Lercher G., Kerber F., Weinberger R., 1996, A&AS 117, 369 (Paper III)
Lu N.Y., Freudling W., 1995, ApJ 449, 527
Lynds B.T., 1968, Stars and Stellar Systems VII, 119
Seeberger R., Huchtmeier W.K., Weinberger R., 1994, A&A 286, 17
Seeberger R., Saurer W., Weinberger R., 1996, A&AS 117, 1 (Paper II)
Weinberger R., 1980, A&AS 40, 123
Weinberger R., Saurer W., Seeberger R., 1995, A&AS 110, 269 (Paper I)

Table 1. Optically detected galaxies in the region $130° \leq \ell \leq 180°$, $|b| \leq 5°$

ZOAG	α(B1950.0)	δ(B1950.0)	α(J2000.0)	δ(J2000.0)	POSS	x(mm)	y(mm)	$\mathcal{D}'$ E		$\mathcal{D}'E_b$	$\mathcal{D}'$ O		$\mathcal{D}'O_b$	cross id.
G130.00+3.61	01 56 40	+65 17.4	02 00 26	+65 31.9	878	142.9	112.9	0.22	0.11		0.22	0.06		
G130.00+3.60	01 56 38	+65 16.7	02 00 24	+65 31.2	878	143.1	112.3	0.17	0.06					
G130.02+3.63 :	01 56 56	+65 18.1	02 00 42	+65 32.6	878	141.5	113.6	0.11			0.06			
G130.09−3.97	01 42 34	+57 53.4	01 45 55	+58 08.4	1240	113.7	33.3	0.11			0.22			
G130.11−4.34	01 42 10	+57 31.5	01 45 30	+57 46.5	1240	116.0	13.8	0.22	0.11	0.06	0.11		0.06	
G130.24−4.18	01 43 21	+57 39.1	01 46 42	+57 54.1	1240	107.7	20.8	0.34	0.22		0.17			
G130.29+1.65	01 54 41	+63 19.4	01 58 20	+63 34.0	878	152.1	7.6	0.06			0.06			WEIN17[1]
G130.46+4.94	02 04 29	+66 26.4	02 08 23	+66 40.6	878	102.9	176.1	0.11						
G130.53−4.92	01 44 16	+56 52.3	01 47 36	+57 07.2	1245	288.3	307.0	0.34	0.22		0.34	0.22		CGCG559-02
G130.53−2.17	01 48 53	+59 33.5	01 52 20	+59 48.3	1240	73.9	124.3	0.22	0.11		0.22	0.11		
G130.65−4.10	01 46 27	+57 38.9	01 49 49	+57 53.8	1240	85.5	21.6	0.11			0.11			
G130.72−4.19	01 46 50	+57 32.6	01 50 12	+57 47.5	1240	82.5	16.0	0.11			0.11			
G130.76−3.62	01 48 04	+58 05.6	01 51 27	+58 20.4	1240	75.3	45.8	0.22	0.17		0.22	0.17		
G130.77−2.84	01 49 32	+58 51.0	01 52 58	+59 05.8	1240	67.3	86.8	0.22	0.06		0.11	0.06		
G130.78−2.67 :	01 49 53	+59 00.8	01 53 19	+59 15.6	1240	65.4	95.6	0.17		0.06	0.11		0.06	
G130.81+4.49 :	02 06 32	+65 54.8	02 10 26	+66 08.9	878	90.1	148.6	0.22	0.11					
G130.86−4.00	01 48 11	+57 41.7	01 51 34	+57 56.5	1240	73.3	24.7	0.11			0.06			
G130.92−4.09	01 48 25	+57 35.8	01 51 48	+57 50.6	1240	71.3	19.5	0.11	0.06		0.22	0.06		
G131.04−4.20 :	01 49 09	+57 27.6	01 52 32	+57 42.4	1240	65.7	12.4	0.11			0.11			
G131.13+3.11	02 05 35	+64 30.1	02 09 23	+64 44.3	878	90.5	73.1	0.11			0.11			
G131.23−2.27	01 54 05	+59 17.6	01 57 33	+59 32.2	1240	37.7	112.4	0.67	0.17	0.11	0.22			
G131.24−3.49 :	01 51 52	+58 06.0	01 55 17	+58 20.7	1240	48.5	47.8	0.11			0.06			
G131.30−2.27 :	01 54 38	+59 16.2	01 58 07	+59 30.8	1240	33.9	111.5	0.11						
G131.30−3.45	01 52 21	+58 07.8	01 55 46	+58 22.5	1240	45.2	49.6	0.22	0.06					
G131.32+4.61	02 11 36	+65 52.1	02 15 32	+66 06.0	878	62.3	148.4	0.45	0.22		0.34	0.13		IRAS02115+6552
G131.42−4.18	01 51 54	+57 23.4	01 55 18	+57 38.1	1245	231.6	332.5	0.56	0.28		0.45	0.11		
G131.48−3.04	01 54 28	+58 28.8	01 57 55	+58 43.4	1240	31.7	69.3	0.17	0.11		0.22	0.11		
G131.70−3.20	01 55 46	+58 16.0	01 59 13	+58 30.5	1240	21.6	58.7	0.11	0.11					
G131.72+3.49 :	02 11 55	+64 40.7	02 15 47	+64 54.6	878	55.0	85.2	0.28	0.17		0.10			
G131.81−4.28	01 54 30	+57 11.6	01 57 54	+57 26.2	1245	212.8	321.5	0.67	0.56	0.34	0.45	0.22		5Zw153[2]
G131.90−4.33	01 55 04	+57 07.5	01 58 28	+57 22.1	1245	209.0	317.8	0.17	0.11		0.22	0.11		
G131.91−4.09	01 55 36	+57 21.5	01 59 01	+57 36.1	1245	204.9	330.3	0.17	0.06		0.11	0.06		
G131.92−4.22	01 55 24	+57 13.7	01 58 49	+57 28.3	1245	206.5	323.4	0.11			0.09			
G131.92−3.09	01 57 34	+58 19.1	02 01 02	+58 33.6	1240	9.3	62.4	0.17		0.06	0.11			
G131.96−2.23	01 59 38	+59 08.2	02 03 08	+59 22.6	597	307.4	110.4	0.11						
G132.00+1.86	02 09 42	+63 02.8	02 13 27	+63 16.8	597	230.8	315.4	0.22	0.11					
G132.01−4.18	01 56 08	+57 14.6	01 59 33	+57 29.1	1245	201.2	324.1	0.17			0.11	0.03		
G132.13−4.65	01 56 05	+56 45.6	01 59 29	+57 00.1	1245	201.8	298.1	0.11			0.11			
G132.14−4.75	01 55 58	+56 39.9	01 59 22	+56 54.4	1245	202.7	293.1	0.22	0.11		0.09			
G132.18−3.99	01 57 41	+57 23.2	02 01 07	+57 37.7	1245	189.9	331.6	0.11						
G132.19+3.50	02 16 02	+64 32.3	02 19 56	+64 46.1	1241	333.6	79.6	0.22						
G132.31−5.00	01 56 39	+56 22.8	02 00 03	+56 37.3	1245	197.8	277.8	0.11			0.22			
G132.37+3.93	02 18 59	+64 53.2	02 22 55	+65 06.8	1241	314.7	96.3	0.11			0.11			
G132.41−4.42 :	01 58 31	+56 54.7	02 01 56	+57 09.2	1245	183.9	306.2	0.11			0.11			
G132.45−3.38	02 00 50	+57 54.1	02 04 18	+58 08.5	597	303.7	43.7	0.39			0.22			MCG+10-04-01
G132.54+3.85	02 20 11	+64 44.9	02 24 07	+64 58.5	878	8.3	93.8	0.11			0.11	0.09		
G132.59−3.20	02 02 14	+58 01.9	02 05 43	+58 16.2	597	293.5	50.1	0.28	0.06		0.03	0.11		
G132.65−4.83	01 59 24	+56 26.8	02 02 49	+56 41.2	1245	177.5	281.3	0.34	0.11		0.22	0.11		
G132.67−3.23	02 02 45	+57 59.2	02 06 14	+58 13.5	597	289.9	47.5	0.17	0.11		0.17	0.11		
G132.68−4.84 :	01 59 33	+56 26.2	02 02 58	+56 40.6	1245	176.3	280.7	0.11		0.06				
G132.76+4.13	02 23 06	+64 56.3	02 27 05	+65 09.8	1241	291.3	96.9	0.34						
G132.90+4.17	02 24 28	+64 55.6	02 28 27	+65 09.0	1241	283.5	95.6	0.22	0.17		0.17	0.11	0.06	
G133.32−4.05 :	02 05 39	+57 00.3	02 09 07	+57 14.5	1245	132.0	311.7	0.22						
G133.47−4.61	02 05 31	+56 26.0	02 08 58	+56 40.2	1245	132.3	281.0	0.12			0.11			
G133.47−4.40 :	02 05 54	+56 38.2	02 09 22	+56 52.4	1245	129.6	292.0	0.22	0.06		0.22	0.06		
G133.48+2.75 :	02 24 45	+63 23.2	02 28 39	+63 36.6	1241	288.3	13.4	0.11						
G133.61−4.68	02 06 16	+56 19.4	02 09 43	+56 33.6	1245	126.5	275.3	0.28	0.11		0.17	0.06		
G133.63−3.61	02 08 48	+57 20.1	02 12 18	+57 34.2	1245	109.6	330.1	0.67	0.45	0.06	0.90	0.45	0.06	
G133.68−4.93	02 06 13	+56 04.0	02 09 40	+56 18.2	1245	126.5	261.6	0.17		0.03	0.17			
G133.83−4.07 :	02 09 10	+56 50.0	02 12 39	+57 04.0	1245	106.0	303.3	0.11			0.11			
G133.83+3.40	02 29 47	+63 51.8	02 33 45	+64 05.0	1241	256.7	36.8	0.56	0.22		0.34	0.17		IRAS02297+6351
G133.84−4.08	02 09 12	+56 49.8	02 12 41	+57 03.8	1245	105.7	303.1	0.10						
G133.87−4.84	02 07 43	+56 05.8	02 11 10	+56 19.9	1245	115.5	263.5	0.22	0.11		0.22	0.11		
G134.02+4.67	02 35 59	+64 57.5	02 40 04	+65 10.4	1241	218.3	93.8	0.34	0.13					IRAS02359+6457
G134.05−4.45 :	02 09 50	+56 24.8	02 13 19	+56 38.8	1245	100.3	281.0	0.11	0.07		0.22	0.11		
G134.15−1.82	02 16 48	+58 52.2	02 20 25	+59 05.9	597	189.9	91.2	0.17	0.06					
G134.19−4.39	02 10 54	+56 25.3	02 14 23	+56 39.3	1245	92.4	281.7	0.22	0.06		0.22	0.11		
G134.22+4.06	02 35 29	+64 19.4	02 39 31	+64 32.3	1241	222.3	59.9	0.17			0.11			IRAS02354+6418*
G134.22+4.05	02 35 25	+64 18.5	02 39 27	+64 31.4	1241	222.7	59.1	0.45	0.11		0.34	0.11		IRAS02354+6418*
G134.69+4.71 :	02 41 53	+64 43.3	02 46 00	+64 55.9	1241	185.1	80.4	0.22	0.06					
G134.70+4.70	02 41 56	+64 42.6	02 46 03	+64 55.2	1241	184.7	79.8	0.34	0.17	0.11	0.22	0.11	0.11	
G134.81−4.07	02 15 54	+56 31.8	02 19 25	+56 45.6	1245	55.8	289.4	0.17			0.17			IRAS02159+5631
G135.01−4.27	02 16 46	+56 16.6	02 20 17	+56 30.3	1245	48.6	276.2	0.22	0.11		0.17	0.11		
G135.06−4.71	02 16 06	+55 50.8	02 19 36	+56 04.6	1617	342.0	260.0	0.17			0.17			
G135.13−4.41	02 17 17	+56 06.0	02 20 48	+56 19.7	1245	44.1	267.0	0.17	0.06					
G135.34−4.08	02 19 28	+56 20.4	02 23 00	+56 34.0	1245	28.8	281.0	0.17			0.11			
G135.40−4.76 :	02 18 13	+55 41.0	02 21 43	+55 54.7	1245	35.7	245.3	0.22	0.06	0.06	0.11	0.06		
G135.61−4.21	02 20 59	+56 07.7	02 24 31	+56 21.3	1617	304.4	272.2	0.17	0.11	0.06	0.17	0.11	0.06	
G135.63−4.27	02 20 58	+56 03.7	02 24 30	+56 17.3	1617	304.7	268.7	0.11	0.06					
G135.66−3.61	02 22 50	+56 40.0	02 26 24	+56 53.5	1617	288.9	300.2	0.11			0.22			
G135.70−3.79	02 22 38	+56 29.6	02 26 11	+56 43.1	1245	6.0	291.1	0.11	0.06		0.17			
G135.71+1.75	02 39 10	+61 36.4	02 43 04	+61 49.1	597	46.3	242.1	0.34	0.11		0.22			
G135.73−4.83	02 20 16	+55 30.0	02 23 46	+55 43.6	1617	312.0	239.1	0.17			0.17			
G135.74−4.83	02 20 16	+55 29.9	02 23 46	+55 43.5	1245	19.5	236.5	0.22	0.11		0.22	0.11		
G135.74−4.53	02 21 03	+55 47.1	02 24 34	+56 00.7	1245	14.7	252.3	1.12	0.90					

[1] IRAS01546+6319 [2] IRAS01546+5711.